Published in final edited form as:
Traffic. 2009 February ; 10(2): 218–234. doi:10.1111/j.1600-0854.2008.00853.x.

α–Synuclein and PolyUnsaturated Fatty Acids Promote Clathrin Mediated Endocytosis and Synaptic Vesicle Recycling

Tziona Ben Gedalya[1], **Virginie Loeb**[1], **Eitan Israeli**[1], **Yoram Altschuler**[2], **Dennis J. Selkoe**[3], and **Ronit Sharon**[1]

[1] Department of Cellular Biochemistry and Human Genetics, Faculty of Medicine, Hebrew University, Ein-Kerem, Jerusalem 91120, Israel

[2] Department of Pharmacology, School of Pharmacy, Hebrew University, Ein-Kerem, Jerusalem 91120, Israel

[3] Center for Neurologic Diseases, Harvard Medical School and Brigham and Women's Hospital, Boston, MA, USA

Abstract

α-Synuclein (αS) is an abundant neuronal cytoplasmic protein implicated in Parkinson's disease (PD), but its physiological function remains unknown. Consistent with its having structural motifs shared with class A1 apolipoproteins, αS can reversibly associate with membranes and help regulate membrane fatty acid (FA) composition. We previously observed that variations in αS expression level in dopaminergic cultured cells or brains are associated with changes in polyunsaturated fatty acid (PUFA) levels and altered membrane fluidity. We now report that αS acts with PUFAs to enhance the internalization of the membrane-binding dye, FM 1-43. Specifically, αS expression coupled with exposure to physiological levels of certain PUFAs enhanced clathrin-mediated endocytosis in neuronal and non-neuronal cultured cells. Moreover, αS expression and PUFA enhanced basal and evoked synaptic vesicle endocytosis in primary hippocampal cultures of wt and genetically depleted αS mouse brains. We suggest that αS, and PUFAs normally functions in endocytic mechanisms and are specifically involved in synaptic vesicle recycling upon neuronal stimulation.

Keywords

α-Synuclein; membrane trafficking; clathrin mediated endocytosis; synaptic vesicle recycling; membrane fluidity; PolyUnsaturated Fatty Acids; Parkinson's Disease

Introduction

The neuronal protein, α–synuclein (αS), has been implicated in the pathogenesis of Parkinson's disease (PD) at both the genetic and cytopathological levels (1–7). Despite the involvement of this abundant neuronal protein in sporadic and familial forms of PD and related α-synucleinopathies, both its normal function and the mechanism by which it gradually accumulates in dopaminergic and other neurons in disease remain unclear.

A portion of αS associates with membranes in vitro (8–16) and in vivo (17–22). These observations are consistent with its primary structure, which contains six imperfect

Corresponding author: Ronit Sharon, Department of Cellular Biochemistry and Human Genetics, School of Medicine, Hebrew University, Ein-Kerem Jerusalem 91120, Israel. Tel: 972 2 675 8170; Fax: 972 2 641 5848; email: ronitsh@ekmd.huji.ac.il.

apolipoprotein A1-like repeats in its N-terminal region that may mediate lipid binding (23,24). We obtained evidence that αS can associate with polyunsaturated fatty acids (PUFAs) in vitro and in neuronal cells and brain tissue (18). Importantly, we found that changes in αS expression can affect membrane and cytosolic PUFA composition and alter membrane fluidity. Specifically, we observed higher levels of certain long-chain PUFAs and higher fluidity in membranes of MES 23.5 dopaminergic cells overexpressing αS than in those of parental cells, and lower levels of such PUFAs and lower fluidity in membranes of αS −/− than normal mouse brains (25). More recently, it was reported that αS can affect brain lipid metabolism and specifically PUFA metabolism (26–29) (30). In agreement with our initial observation that αS expression affects membrane FA composition (25), these studies in αS null mouse brains documented reduced incorporation of certain FAs into membrane phospholipids as well as decreases in FA uptake and turnover (26,27,30,31).

During endocytosis, a small region of the plasma membrane invaginates to form a new intracellular vesicle containing various cargo molecules. Clathrin-mediated endocytosis (CME) is the major entry route for extracellular molecules such as nutrients, hormones and signaling factors and serves to regulate the internalization of trans-membrane receptors, including the recycling of pre- and postsynaptic neuronal membrane proteins (32–34). Although clathrin coated vesicles are found in all eukaryotic cells, their components are particularly enriched in brain, where clathrin and its partner proteins are implicated in the biogenesis of presynaptic vesicles, the major secretory organelles within the nervous system (35,36). The cargo for endocytosis is usually recognized by a specific receptor on the cell surface. Most receptor-mediated endocytosis (RME) is mediated by clathrin coated pits.

PUFAs have been found to play a role in the formation and/or maintenance of synaptic vesicles (37,38), including dopaminergic vesicles (39–44). It has been hypothesized that due to their “cone shape”, PUFAs affect membrane curvature in a way that promotes vesicle budding and membrane trafficking (45,46). In this context, it is of interest that αS is localized in part to presynaptic neuronal terminals, and has been found to be involved in the genesis and/or maintenance of the reserve, or resting, presynaptic vesicle pools (17,47,48).

Here we assess the effects of αS and PUFAs on plasma membrane trafficking. We provide evidence that αS and PUFAs affect endocytosis and vesicle recycling in both neuronal and non-neuronal cells and specifically activate synaptic vesicle recycling after neuronal stimulation by enhancing CME.

Results

αS occurs in soluble oligomers and affects the cellular incorporation of ^{14}C oleic acid

We previously reported that a portion of cellular αS can be detected as low-n soluble oligomers (dimers up to hexamers) (49). However, the visualization of these SDS-stable oligomers on Western blots required pre-extraction of lipids, for example by heating cytosolic or membrane fractions to 65°C or else, performing chloroform/methanol extraction. Such treatments could potentially induce protein denaturation and aggregation in the presence of SDS sample buffer. To address whether the lipid-associated soluble αS oligomers occur under non-denaturing conditions in vivo, we have incubated high-speed cytosols (post-100,000g) of mouse brains with Lipidex-1000 (4°C; 16 hr) followed by native gel electrophoresis. This revealed αS forms migrating higher than the monomer in wt mouse brains and to a greater extent in A53T αS +/+ transgenic mouse brains (73) (Fig. 1a). The signal was not present in cytosol from αS −/− mouse brains, confirming its specificity (Fig. 1a). We next analyzed the high-speed cytosols of untransfected and αS-overexpressing MES dopaminergic cells grown in serum-free medium supplemented with 35 μM ^{14}C oleic acid (OA) and 35 μM FA-free BSA (a known FA carrier protein) for 16 hr followed by native gel

electrophoresis. The αS-overexpressing cells incubated under these conditions consistently showed greater amounts of ^{14}C OA incorporation throughout the lane than did untransfected naive cells (Fig. 1b). We conclude that cytosolic αS occurs natively in the form of soluble oligomers and affects the cellular fatty acid content.

αS enhances the internalization of FM1-43 labeled plasma membrane

To assess the possible involvement of αS in membrane trafficking, we initially used the well-characterized lipophilic dye, FM1-43 (reviewed in (50,51)), to detect newly formed endocytic vesicles budding from the plasma membrane of MES dopaminergic neuronal cells maintained in standard serum-supplemented medium. FM1-43 (2.5μM) was added to the conditioning medium for 4 min at 37°C, and then free dye was removed by multiple washes. The labeled cells were then cultured at 37°C for an additional 30 min to allow endocytosis. Higher levels of FM1-43 labeled endocytic vesicles were invariably detected by confocal microscopy in cells stably overexpressing human wt αS than in non-transfected MES cells maintained under standard serum conditions (Fig. 2a). Quantifying the FM1-43 signal revealed a ~10 fold increase in wt αS over expressing cells than parental MES cells. This increase in FM1-43 internalization correlates with the ~13 fold increase in αS expression vs. naive untransfected cells. In quantitative experiments employing similar levels of αS expression and identical FM1-43-containing medium, stable expression of the PD-causing A53T αS mutant induced a more marked effect (2–3 times wt levels) in the amount of internalized FM1-43 labeled membrane (Fig. 2a).

In view of our earlier findings that increased cellular PUFA levels enhance αS oligomerization (49) and that αS expression levels affect cellular PUFA composition (25), we next asked whether PUFAs play a role in the accumulation of αS-dependent, FM1-43 labeled endocytic vesicles. For this, we conditioned naive- and αS-overexpressing MES cells in serum-free medium supplemented with BSA only (50 μM) or with BSA plus the 18:3 PUFA (250 μM) (see Methods). The cells were conditioned in the specified medium for 16–18 hr prior to labeling with FM1-43 (as described above), and the effects on endocytic vesicle formation were again observed by confocal microscopy. A consistent increase in FM1-43 fluorescence was detected in wt αS overexpressing cells conditioned in serum-free medium supplemented with BSA only, specifically, an increase of ~7 fold over the parental, naive cells (Fig. 2b). Thus, the effect of αS overexpression in enhancing endocytosis can be seen in the absence of any exogenous lipids in the conditioning medium. An increase in intracellular FM1-43 fluorescence was detected in parental cells conditioned in BSA + 250 μM 18:3 (increased ~5 fold vs. BSA alone) (Fig. 2c). Thus, the effect of PUFA on endocytosis can occur independently of αS expression. Further, a marked enhancement of plasma membrane internalization was observed by combining wt αS overexpression with 250 μM 18:3 (increased ~30 fold vs. parental MES cells conditioned in BSA alone, i.e., no 18:3 and no αS) (Fig. 2d). The combined effect of αS stable expression and 18:3 was far higher than the addition of the effects of each factor alone, suggesting that PUFAs and αS act synergistically in this assay. Further enhancement in FM1-43 fluorescence was observed in MES cells stably expressing the A53T αS and conditioned in medium supplemented with BSA or BSA-PUFA (Fig. 2b–d). Importantly, the fold-increase (vs. serum-free medium) of plasma membrane internalization in standard serum containing medium or in medium supplemented with a PUFA (i.e., BSA + 250 μM 18:3) was closely similar. That is, an increase of ~10 and ~12 fold was detected with standard serum and with PUFA, respectively, in αS over-expressing cells (see Figs. 2a and c). This closely similar effect of serum and a single PUFA indicates that the substantial response of the cells to a concentration of 250 μM 18:3 is in a physiological range. Nevertheless, we next performed this experiment at a lower concentration of 100 μM 18:3 and obtained similar results but with a lower-fold induction; again, αS or PUFA alone each induced FM1-43 internalization,

and they showed an apparent synergistic effect upon their combination (Fig 2e). Finally, we performed western blot analyses of wt and A53T αS overexpressing cells and detected similar αS expression level in both clones (Fig. 2f). Importantly, we tested FM1-43 internalization as a function of expression of the related family member, βS, and found no effect of βS expression alone or when combined with 18:3 treatment.

We next compared the effects of αS expression in neuronal and non-neuronal cell lines to determine whether the effect was restricted to neuronal cells. We examined HeLa, HEK 293, SK-N-SH, MN9D and MES cells, the two latter being dopaminergic neuronal lines. In all five cell lines, αS expression consistently and markedly enhanced the levels of internalized FM1-43 labeled membrane (not shown). We conclude that the robust effect of αS expression in enhancing the internalization of FM1-43 labeled plasma membrane is not specific to neuronal cells and can be observed in other cell types upon its overexpression.

PUFAs of greater carbon chain length and higher degree of unsaturation are more potent in inducing αS-dependent endocytosis

To confirm and extend the effects of 18:3 on the accumulation of endocytic vesicles, we compared the effects of different FAs on the formation of FM1-43-labeled vesicles in the presence of αS overexpression. Intriguingly, the saturated FAs (SFA), 18:0 and 20:0 (each at 250 μM, with 50 μM BSA as the standard carrier protein) decreased the accumulation of FM1-43 labeled endocytic vesicles compared to BSA only. The MonoUnsaturated Fatty Acid (MUFA), 18:1, produced no detectable alteration compared with BSA alone and longer chain MUFA, 20:1, slightly but significantly enhanced the accumulation of FM1-43. In contrast, the PUFAs, 18:2, 18:3, 20:2, 20:3 and 20:4, each consistently induced the accumulation of FM1-43 endocytic vesicles (Table 1). We found that the quantitative effect of PUFAs on the FM1-43 internalization signal varied as a function of both increasing carbon chain length and increasing degree of unsaturation. The longer and more polyunsaturated the FA, the more FM1-43 fluorescently labeled endocytic vesicles accumulated inside the cells (Fig. 3 and Table 1). In general, the vesicles appeared larger and more coalesced after treatment with the longer, more unsaturated FAs vs. with BSA alone.

αS and PUFAs enhance endocytosis of transferrin

To elucidate the type of endocytic mechanism that is activated by αS and PUFAs, we studied the internalization of transferrin (Tf) by the transferrin receptor (TfR), the archetypical cargo for internalization via Clathrin Mediated Endocytosis (CME), as a model for Receptor-Mediated Endocytosis (RME). TfR binds its ligand (ferrotransferrin) at the cell surface and is internalized into early endosomes, where it releases the bound iron and recycles back to the plasma membrane. To measure the effects of αS and PUFAs on Tf endocytosis, we used fluorescently-labeled human Tf (Alexa-488-Tf). MN9D cells were conditioned in serum-free DMEM supplemented with BSA +/− 18:3 or 18:1 (50 and 250 μM for BSA and 18:3 respectively) for 16 hr, followed by the application of Alexa 488-Tf (50 μg/ml) at 4 °C for 60 min to allow the binding of Tf to its receptor without internalization. Cells were then washed and transferred to 37 °C to allow internalization, fixed in 4% PFA and processed to visualize and quantify Alexa-488-Tf by confocal microscopy (see Methods).

Using the naive, untransfected MN9D cells supplemented with BSA only (at 50 μM) as the control for basal endocytic activity, we found that 18:3 by itself (at 250 μM) induced Tf endocytosis into large endosomal vesicles (Fig. 4a, b). αS overexpression alone also induced Tf endocytosis, resulting in a diffuse pattern of many smaller endocytic vesicles. The combination of αS overexpression and 18:3 in the conditioning medium further enhanced

endocytosis of fluorescent Tf by the receptor (Fig. 4a, b). Importantly, the corresponding 18:1 treatment had no effect on Tf endocytosis, (not shown). We performed the same experiments in MES dopaminergic cells and neuroblastoma SK-N-SH cells, yielding very similar results (not shown). Additionally, we tested the effect of αS expression on Tf endocytosis in the presence of standard serum-supplemented conditioning medium and found that the PUFA activation of Tf endocytosis is within the physiologic range of serum alone (Fig. 4b).

We next measured Tf endocytosis as a function of increasing 18:3 concentrations in the SK-N-SH cells with or without αS overexpression. A dose-dependent effect of 18:3 concentrations on degree of Tf endocytosis was detected in naive and αS over expressing cells (Fig. 4c). Higher degree of endocytosis was detected in αS over expressing cells throughout the 18:3 range of concentrations up to the highest concentration tested, i.e. 250 μM (Fig. 4c). Importantly, the increased slope in αS over expressing (a=0.13) vs, naive cells (a=0.06) suggests that αS and 18:3 may act synergistically. A significant increase in endocytosis of Tf was detected already at the lowest 18:3 concentration tested (i.e. 50 μM, ttest, $P<0.05$), which is well within the physiological range of brain PUFA concentrations (52). Increased levels of Tf endocytosis were detected in a linear relationship to the increased 18:3 concentrations, with a correlation coefficient of 0.96 ($p<0.001$, not shown).

αS and PUFAs affect TfR cellular distribution and expression level

We examined the protein levels and cellular distribution of TfR in naive and αS over expressing cells. MN9D cells were incubated in serum free DMEM (to obtain low iron levels) and supplemented with BSA and 18:3 for 16–18 hr, as above. Following the addition of Tf (see above) cells were fixed in 4% PFA and processed for icc with an antibody to TfR to determine receptor level and distribution. Using naive MN9D cells supplemented with BSA only(50μM) as the control for basal TfR level and cellular distribution, we found that adding 18:3 (250 μM) or over expressing αS resulted in quantitative increases in total receptor signal at the cytoplasm and the cell surface, with further enhancement of TfR signal by combining αS and PUFA (Fig. 5a).

We next performed surface biotinylation experiments to confirm the apparent increase in cell-surface TfR levels. Naive and αS over expressing MN9D cells were conditioned in serum-free medium supplemented with BSA +/− 18:3 (at 250 μM) for 16 hr. Cells were then transferred to 4°C to prevent internalization of receptors. Cell surface proteins were biotinylated with sulfo-NHS-LC-biotin (0.5 mg/ml). The amount of biotinylated TfR was normalized to the amounts of total TfR protein levels and to actin in the same sample using quantitative western blotting. A higher portion of surface TfR was detected upon αS expression or PUFA treatment, with highest surface TfR ratios detected in the αS over expressing PUFA-treated cells (Fig. 5b). The effect of αS expression on surface TfR levels was also determined under standard serum-supplemented conditioning medium with very similar results (Fig. 5b).

Densitometry of western blots probed with anti TfR antibody showed elevated total TfR protein in response to PUFA treatment alone (~60% increase), to αS overexpression alone (~85% increase) or to both combined (~200 % increase) (Fig. 5b). In accord, we detected a ~ 3 fold increase in TfR mRNA levels in the αS over expressing cells compared with the naive cells (Fig. 5c) conditioned in standard serum-supplemented medium. Marked increases in TfR mRNA levels were detected in the BSA and PUFA treated cells. These may result from the effect of serum starvation and low iron levels; nevertheless, under these serum-free conditions, the levels of TfR mRNA were higher (but not significantly higher) in the PUFA-treated than BSA-treated cells (Fig. 5c). Therefore, αS expression enhanced TfR expression,

and combining αS expression and PUFA treatment resulted in a further increase in TfR expression.

αS and PUFA enhance the rate of TfR internalization and recycling

Using Alexa-488 Tf, we next measured αS and PUFAs effects on the rates of internalization and recycling of TfR. Naive and αS overexpressing MN9D cells were conditioned in serum-free medium supplemented with BSA +/− 18:3 (at 50 μM BSA and 250 μM 18:3) for 16 hr. We were concerned that comparing cellular membrane trafficking of cells treated in BSA only vs. with PUFA was not ideal. We therefore performed the experiment comparing the effects of 18:1 and PUFA (18:3). Nevertheless, no difference was found between the effects BSA and 18:1 on TfR recycling (not shown). To measure internalization, cells were incubated with Alexa-488 Tf (25 μM) for the indicated times, surface bound Alexa-488 Tf was then removed by acid wash, and internalized Alexa-488 Tf was measured using flow cytometry (FACS analyses) (Fig. 6a). The results suggest that αS alone or PUFA alone increase the rate of internalization, with the highest rate of internalization observed in αS overexpressing cells treated with PUFA. Internalization rate constants (calculated as internalized fluorescent per minute) are: 2.05 (R^2=0.92) and 3.05 (R^2= 0.91) for naive cells treated with BSA and PUFA respectively, and 3.09 (R^2=0.85) and 4.7 (R^2= 0.89) for αS over expressing cells treated with BSA and PUFA respectively. Two way ANOVA indicated significant differences between the curves (Fig. 6a) and the post hoc Student-Newman Keuls test indicated a significant effect for αS expression, PUFA treatment and the combined αS and PUFA ($p<0.05$). Interestingly, the internalization of transferrin in naive cells with 18:3 and in αS cells with 18:1 was highly similar, suggesting that either αS expression or PUFA treatment on their own, enhances transferrin endocytosis to the same levels.

To measure TfR recycling, Alexa-488 Tf (25 μM) was loaded for 60 min at 37 °C to reach steady state. Excess unbound Alexa-488 Tf was then removed by washes, and cells were further incubated at 37 °C for the indicated times (Fig. 6b). Enhanced recycling is observed when combining αS expression and PUFA treatment and to a lesser extent with each treatment on its own. Recycling rate constants (calculated as internalized fluorescence per minute) are −0.032 (R^2=0.86) and −0.035 (R^2= 0.85) for naive cells treated with BSA and PUFA respectively, and −0.045 (R^2=0.92) and −0.055 (R^2= 0.82) for αS over expressing cells treated with BSA and PUFA respectively. Two way ANOVA indicated a significant effect for αS expression on the rate on recycling ($p<0.05$). However, the effects of PUFA on recycling were not significant.

In accord with the increased TfR levels at the cell surface, Tf binding assays at 4°C (to allow binding but not internalization), showed increased Tf binding to the cell surface TfR (not shown). Specifically, considering naive MN9D cells treated with BSA only as a control for basal Tf binding to the surface receptors, either 18:3 treatment or αS over expression resulted in enhanced levels of bound Tf, with the maximal level of surface bound Tf observed in αS over expressing cells treated with 18:3 PUFA (not shown).

Taken together, the enhanced binding to TfR, enhanced levels of cell surface TfR and enhanced rate of internalization all act to increase Tf endocytosis in the presence of PUFA, αS or both.

αS and PUFA enhanced endocytosis is mediated by clathrin

In light of our recent findings suggesting αS involvement in affecting PUFA membrane composition and membrane fluidity (25), we sought to exclude the remote possibility that αS and PUFA induce Tf endocytosis through an alternative RME mechanism. To verify that αS- and PUFA- induced Tf endocytosis is mediated by CME, we treated naive and αS

overexpressing dopaminergic MN9D cells with BSA (50 μM) or BSA + 18:3 (250 μM) for 16 hr and determined clathrin protein level by western blot probed with anti-clathrin or anti-actin antibodies. Densimetric analyses of the clathrin heavy chain normalized to actin on the same blot indicated increases in clathrin protein levels by αS expression, by PUFA and much further by combining them (~ 40%, 60% and 200% increases, respectively; Fig 7a). A similar result was observed by icc with increases in clathrin signal and in accord, transferrin signal, upon either αS over expression or PUFA treatment with highest signals observed by combining αS and PUFA (Figure 7b left panel). Quantifying clathrin and transferrin signals suggests a correlation between the increases in clathrin and transferrin (Fig. 7c). Considering naive cells treated with BSA as control, we found that transferrin internalization and clathrin expression were both significantly increased by either PUFA treatment or αS over expression and further by αS and PUFA combined (ANOVA $p<0.001$). These data support the conclusion that the increase in Tf internalization signal invariably observed with αS and PUFA (Figs. 4 and 6a) results from activation of CME.

As an alternative approach to confirm the involvement of clathrin in αS- and PUFA- induced endocytosis, we designed an shRNA to inhibit the expression of the clathrin heavy chain and thereby the assembly of clathrin (53). We selected an shRNA duplex that targeted the segment 4643–4663 of the mouse clathrin heavy chain open reading frame and inserted it into the Plko.1 plasmid (see Methods). Clathrin shRNA and unmodified Plko.1 plasmids were transfected into naive and αS overexpressing dopaminergic lines MES and MN9D with indistinguishable results (not shown). Thirty two hours after transfection of the siRNA, the cells were transferred to conditioning medium (serum-free) supplemented with BSA +/− 18:3 (50 and 250 μM, respectively) and maintained under these conditions for 16 hr. Then (48 hr after transfection), the cells were assayed for clathrin levels and Alexa-488 Tf endocytosis by icc or western blotting.

To quantify the reduction in clathrin heavy chain expression, the transfected cells were extracted and blotted for clathrin heavy chain (and tubulin as a loading control). A sharply reduced level of clathrin heavy-chain was detected in the cells transfected with clathrin siRNA vs. cells transfected with empty plasmid or left untransfected, whereas tubulin was unchanged. Quantification of αS over expressing MES cells transfected with the clathrin shRNA or empty Plko.1 and treated with 18:3 PUFA showed that the cellular concentration of clathrin heavy chain had dropped to ~27% of control levels (Fig. 7d). In accord, reduced clathrin expression throughout the cell was found by icc in the siRNA vs. mock transfected cells (Fig. 7b right panel, 7e) accompanied with reduced Tf endocytosis in the clathrin siRNA-transfected but not mock transfected cells (Fig 7b,e). The reduced clathrin signal and Tf endocytosis following transfection with clathrin siRNA was observed in all four combinations of αS expression and PUFA, i.e., naive cells treated with BSA or PUFA and in αS over expressing cells treated with BSA or PUFA. (with ~60–90% reduced signal throughout the treatments).

We next confirmed these results with a second shRNA that targeted the segment of 3387–3408 of the clathrin heavy chain vs. its scrambled sequence. The results indicated that the clathrin siRNA but not its scrambled sequence reduced clathrin expression throughout the cell and reduced Tf endocytosis by ~ 65% in αS over expressing cells treated with PUFAs (not shown).

αS expression and PUFA treatment enhance endocytic vesicle formation in primary neurons

αS is a presynaptic protein believed to be involved in synaptic vesicle (SV) generation and/or maintenance (47,48). To determine whether the striking effects of αS plus PUFA exposure pertain to synaptic activity, we again used the lipophilic dye, FM1-43. This dye

has been used extensively in diverse experimental systems to study mechanisms involved in synaptic vesicle recycling (reviewed in (51) (54,55)). The concept behind using FM1-43 to assess synaptic and endocytic vesicles is similar. In both cases, FM1-43 is a marker for plasma membrane internalization. Further, it is well established that SV formation is mediated by CME (reviewed in (35,56)).

Primary hippocampal neurons (18 days in vitro) from normal and αS null (−/−) mouse brains were grown in serum-free medium supplemented with BSA +/− 18:3 (10 and 50 μM respectively) for 16 hr prior to membrane depolarization with KCl (70 mM for 60 sec), and synaptic vesicle formation was analyzed in the presence of FM1-43 (10 μM). Neurons were rinsed of excess FM1-43, fixed and processed for icc with anti-synaptophysin antibody as a marker for synapses (Fig. 8). The chemical stimulation resulted in uploading the fluorescent dye into the hippocampal neurons. We also performed this experiment with an even lower 18:3 concentration (25 μM) with very similar results (not shown).

Overall, we detected higher levels of FM1-43 dye in synaptic terminals in the neuropils of wt than αS −/− mouse hippocampal cultures exposed to BSA alone, and then saw a substantially more pronounced induction upon exposure of the cultures to PUFA (Table 2 and Fig. 8a). Importantly, each factor alone, i.e., αS expression or 18:3 treatment, induced FM1-43 uptake into SV, indicating that they can act independently of each other to enhance new synaptic vesicle formation (Fig. 8a). However, the number and size of synaptic puncta were higher in the hippocampal neurons from wt mouse brain treated with 18:3, again indicating at least an additive effect between αS expression and PUFA levels. Further, these results suggest that either αS −/− synapses maintain a smaller pool of SV or that the recycling of the vesicles in αS −/− synapses is delayed.

In accord with the reduced FM1-43 signal, we detected reduced signal for synaptophysin in the αS −/− synaptic terminals (Table 2, Fig. 8b). Specifically, we detected reduced synapse size and reduced intensity of synaptophysin signal in the αS −/− neurons. Quantifying the total synaptophysin signal per cell revealed that the signal in αS −/− neurons was ~58 % lower than the signal detected in the wt neurons. However, no significant effect for PUFA on synaptophysin signal was detected by icc (Table 2) or quantitative western blotting (not shown). Further, to determine FM1-43 uptake specifically into boutons, we calculated the percent of synaptophysin-positive boutons that were also positive for FM1-43. We found that ~40 and ~75% of synaptophysin-positive boutons were also positive for FM1-43 in wt cultures treated with BSA and BSA + PUFA, respectively, indicating that PUFA- induced FM1-43 internalization occurs into synaptic pools at the synapses. Nevertheless, a substantial amount of the PUFA-induced FM1-43 internalization signal appeared along the neurite and not within synaptic terminals or boutons (i.e., was not co-localized with synaptophysin). This result indicates that PUFA-induced internalization is not restricted to SV at synaptic pools. In αS −/− neurites, we observed that PUFA alone induced FM1-43 internalization into synaptic terminals as well as into SV along the neurite. However, due to the lower number of synaptophysin-positive boutons in the αS −/− neurites, we found that ~60 and ~95 % of the synaptophysin-positive boutons were positive for FM1-43 in the BSA and BSA + PUFA treated cultures, respectively.

Next, the primary cultures were depolarized in KCl one more time, to down load the FM1-43 dye from the SV (see Methods). This second cycle of depolarization with KCl now evoked exocytosis of the FM1-43 loaded SV and therefore resulted in a markedly reduced fluorescent signal, confirming FM1-43 downloading by evoked SV recycling (Fig 8c). We conclude from these results that the FM1-43 dye is internalized specifically into SV.

A similar increase in FM1-43 uptake into vesicles was also observed in the neuronal cell bodies. Consistent with the increased FM1-43 internalization into SV, this increase is dependent on αS expression and the presence of PUFA (Fig. 8d). However, this internalization of FM1-43 dye into neuronal cell bodies occurred without chemical depolarization of neurons. Further, this FM1-43 signal was not washed out with a subsequent depolarization and did not co-localized with synaptophysin. This result suggests the possible involvement of αS expression and PUFA in constitutive mechanisms of neuronal endocytosis.

Very importantly, no induction of FM1-43 uptake was observed at either the somata or neurites when hippocampal neurons from wt and αS −/− mice were conditioned in the presence of 18:1 (50 μM), performed in parallel to the 18:3 experiments (data not shown). This control indicates that PUFAs, but not MUFAs of identical carbon chain length are capable of activating these endocytic mechanisms.

Discussion

Taken together, these experiments provide new evidence that αS and PUFAs can act in at least an additive fashion to modulate membrane trafficking, with a specific focus on their individual and combined effects on endocytosis mediated by clathrin. Overall, we found that αS expression or PUFA treatment induced endocytosis, with further induction upon their combination. In general, at the same carbon chain length and concentration, PUFAs induced and SFAs inhibited endocytosis. MUFAs effect on induced endocytosis was milder and was observed only with the longer carbon chained FAs. Using the canonical example of ligand internalization through receptor-mediated endocytosis, we show that αS and PUFA induce the endocytosis and recycling of Tf by the TfR. αS and PUFA-induced Tf endocytosis is molecularly specific, as it is inhibited by clathrin siRNA. Relevant to the physiological function of αS in the brain, our findings indicate that αS and PUFAs can act together to stimulate SV formation in primary hippocampal neurons. Specifically, αS is implicated in the endocytic recycling of SV following neuronal stimulation. Importantly, primary hippocampal neurons genetically deleted of αS showed reduced number and size of synaptophysin-positive boutons and reduced FM1-43 endocytosis in SV, suggesting a reduced recycling pool. Based on these invariant results in primary neuronal cultures, we suggest that αS and PUFA are normally involved in the endocytic machinery leading to SV formation and replenishment and thus synaptic strengthening.

Early reports that αS is localized to nerve terminals (17,57,58) and associates with SV (59) suggested the possible involvement of αS in the formation/maintenance of SV and/or neurotransmitter release. Several subsequent studies have shown that αS expression has a role in the formation or maintenance of distinct synaptic pools. In particular, reduced sizes of distinct synaptic pools in primary hippocampal neurons were observed upon partially silencing αS expression (48) and also in hippocampal neurons from αS −/− brains (47). In accord, increased accumulation of docked vesicles was observed in PC12 cells upon αS overexpression (60). Furthermore, αS has been postulated to be involved in the replenishment of synaptic pools after a depleting stimulation (47). Nevertheless, these various observations were not consistent with certain findings in other αS −/− mouse models. No alterations in synaptic pool size or replenishment of recycling SV were observed in αS −/− mice or in the double-knockout αS −/− and αS −/− mice (61), and αS was suggested to negatively regulate the readily releasable pool of DA-containing vesicles (62). These variations in observations may result from the different mouse models and experimental designs employed and highlight the complexity of synuclein's physiological role. The new results presented herein strongly support a role for αS in the formation/maintenance of SV and/or neurotransmitter release. Furthermore, the results indicate that αS

is involved in mechanisms leading to synaptic strengthening. That is, the reduced number and size of synaptophysin-positive boutons observed in αS −/− neurons indicates lower synaptic activity. This, in turn, could affect the plasticity of neuronal networks that is known to underlie cognitive functions such as learning and memory.

Recent studies have suggested that αS is involved in other aspects of membrane trafficking, possibly in exocytosis or in the secretory pathway. It has been reported that αS expression specifically inhibits ER to golgi trafficking, resulting in cytotoxicity that was prevented by Rab1 expression (63). It was further shown that αS expression affected vesicle docking or fusion to the golgi apparatus after an efficient budding from the ER (64). In PC12 cells, αS overexpression inhibited evoked catecholamine release and increased the “docked” vesicle pool (60). Other studies have suggested an indirect role for αS in promoting the assembly of the SNARE complex (61,65). SNAREs catalyze the fusion of vesicles with their target membranes to enable the release of cargo from the vesicle (reviewed in (66,67)). Collectively, growing evidence implicate αS in membrane trafficking, including endocytosis and exocytosis.

In addition to our observed induction of FM1-43 uptake into SV, α S plus PUFA additively induced dye uptake into neuronal cell bodies. Despite extensive investigation, it remains unclear whether the endocytic pathways at nerve terminals are specializations of the pathways that exist in all cells or rather represent a neuron-specific mechanism for rapid membrane recycling (see e.g., (68)). In this regard, whether neurons have classical endosomes is also unresolved. Therefore, the nature of the induced vesicles we observed in the neuronal cell bodies is yet to be determined. Nevertheless, since we found that αS can activate endocytosis at both neuronal and non-neuronal vesicles, these pathways most likely share a high degree of similarity.

We previously reported that αS expression in cells and brain is associated with enriched levels of certain PUFAs in both the cytosol and membranes, and this was associated with apparent changes in membrane biophysical properties reflected by increased membrane fluidity (25). Our initial working hypothesis after we obtained these results was that the αS effects on membrane fluidity may relate directly to its effects on membrane trafficking. Our rationale was that αS may act to enrich the cytoplasmic membrane leaflet with PUFAs. PUFAs in the membranes act as cone-shaped lipids that induce a positive curvature of the membrane leaflet (45,69), thus inducing invagination and fission of the membrane and thereby enhancing membrane trafficking. The results presented herein support this initial working hypothesis. It is supported by the specific inducing effect of PUFAs (but never MUFAs or SFAs of identical carbon chain length and concentration) -- either with or without αS over expression -- on endocytosis and SV formation. Therefore, we speculate that αS and PUFA mechanically alter membrane curvature as a result of enrichment of the plasma membrane with PUFAs, thereby facilitating endocytosis, including, among other mechanisms, CME.

In addition to the general role of membrane curvature in endocytosis discussed above, the findings herein that αS + PUFAs effects can alter actual protein levels of specific key factors in CME and RME, i.e., TfR and clathrin, and also redirect TfR to the cell surface membrane indicate activation of regulatory mechanisms that may secondarily lead to the over expression or stabilization of these specific endocytic participants. A hypotheticalbiological target for αS/PUFA activation is certain classes of membrane phospholipids, and specifically phosphoinositides, that are known to regulate CME (reviewed in (70)). Further investigation will be needed to elucidate the specific molecular mechanisms by which αS and PUFAs activate endocytosis.

We view the data we have obtained to date as addressing a normal physiological role of αS. On the other hand, it is likely that there are pathophysiological implications of our findings. For example, we observed that the accumulation of αS into high MW assemblies, including soluble cytosolic dimers and low-n oligomers that could well serve as the nidus for αS aggregation into Lewy-type fibrillar deposits, is associated with alterations in neuronal PUFA composition. That is, we examined FA profiles in mesencephalic neuronal cells that stably express αS and found accumulation of PUFAs in cytosols as well as membrane fractions in such cells, compared with parental cells that express low levels of endogenous αS. These changes could be relevant to the overexpression of wt αS in PD families with duplication or triplication of the αS locus, and also to idiopathic PD cases that invariably accumulate wt αS in the neuronal cytoplasm. In this regard, it is interesting to consider the correlation between PUFA-induced αS oligomerization (49) and PUFA-induced FM1-43 uptake (herein). In both cases, the longer and more unsaturated the FA, the more αS oligomerization and the more FM1-43 internalization one observes. This correlation may suggest that the soluble, cytosolic oligomers are the active forms.

Collectively, our earlier and current results suggest that αS normally interacts with PUFAs to carry out its physiological functions, but under certain potentially pathogenic conditions, this interaction may lead to neuronal membrane dysfunction and ultimately αS aggregates and cell death. We propose that this shift on a continuum between normal and pathogenic αS-lipid interactions may be driven by transient increases in either the levels of certain PUFAs or the levels of αS monomers in the cytoplasm.

Materials and Methods

Cells

The mesencephalic neuronal cell lines MES 23.5 and MN9D which have dopaminergic properties (71,72), were stably transfected with wt human αS cDNA in the pCDNA 3.1 vector using Lipofectamine 2000 (Invitrogen CA, USA). A reported feature of the αS-transfected MES cells was that all stable clones gradually lost αS expression after being continuously passaged for 2 3 months or more (18). To overcome this technical problem and increase consistency of results, we kept frozen aliquots of MES and MN9D αS over expressing clones. The clones were frozen at 55–65 days post DNA transfection and fresh aliquots were thawed routinely every 4–8 weeks. Experiments performed in SK-N-SH neuronal lines involved viral infection with αS expressing adenovirus (see below).

Detection of αS oligomers and native gel electrophoresis

Normal, αS +/+ (73) and αS −/− (74) mouse brains were homogenized and fractionated as described before (18). Samples (15 μg) of high speed supernatant (post 100,000g) were incubated with Lipidex 1000 (w/vol) for 16 hours. Samples were spun down to remove Lipidex-1000 and the supernatant was loaded on a 10% Tris Glycine polyacrylamide gel (without SDS in gel, running or loading buffers). The proteins were transferred to PVDF membrane and probed with syn-1 antibody (Tranduction Laboratories KY, USA). For the in vivo association of αS with ^{14}C OA, cells were incubated with the indicated mixture of FA and BSA, fractionated as above and samples of high speed supernatant was subjected to native gel electrophoresis as above. The gel was dried and autoradiogram obtained.

FM1-43 internalization into endocytic vesicles

To visualize endocytic membrane trafficking, cells (growing on cover glass of 12 wells) were incubated at the presence of 2.5 μM FM1-43 (Fixable; Molecular Probes, Eugene, OR) for 4 minutes at room temperature. Unbound probe was removed, and the cells were washed twice and re-incubated for 10 minutes at 37°C with the indicated conditioning medium. The

cellswere then washed and fixed with 4% PFA. Cover glass were then either prepared for microscopic analysis to observe FM1-43 fluorescence or else subjected to icc.

Tf binding and endocytosis

Alexa 488-human Tf was purchased from Molecular Probes (Eugene, OR). Cells (SK-N-SH, MES or MN9D) were plated on cover glass coated with 0.01 mg/ml poly-D-lysine the day before experiment. Alexa-488 human Tf (or the equivalent non-fluorescent Tf for icc with TfR antibody) was added to the cells at 50μg/ml in plain DMEM medium without any supplements, in the presence of 0.1 mg/l of $Fe(NO_3)_3*9H_2O$, at 4°C for 60 minutes. Unbound Tf was removed and cells were transferred to 37°C for additional 10 minutes at the indicated conditioning medium, to allow endocytosis. Cells were then fixed with 4% PFA for 10 minutes on ice and either processed for quantitative measurements of internalized Tf or processed for icc with the indicated ab, using secondary cy5-conjogated (emission at 633).

Immunocytochemistry (icc)

Following fixation with 4% paraformaldehyde for 10 minutes on ice, cells were washed and permeabilized with 0.2% Triton X-100 in PBS and 1% goat serum for 5 minutes at room temperature. Slides were then blocked with 1.5% goat serum in PBS. Primary abs: monoclonal mouse anti Clathrin heavy chain (1:250, BD Biosciences NJ USA); monoclonal mouse anti TfR (1:100, Zymed Laboratories CA, USA); monoclonal mouse anti synaptophysin ab (1:200 DAKO, Glostrup Denmark) and secondary ab at 1:200, anti mouse-cy5 (Molecular probes CA, USA); anti mouse-Cy5 (Jackson ME, USA). Slides were sealed with mounting medium (cat# M1289 Sigma Rehovot, Israel) and analyzed by confocal microscopy.

Clathrin shRNA construction

The shRNA for clathrin heavy chain (mouse) was designed according to the Broad Institute, TRC, The RNA consortium website. The shRNA targeting sequence is: GCGAACATCAATAGATGCTTA, total of 21 nucleotides at position 4643–4663. The sequence of the forward primer is: CCGGGCGAACATCAATAGATGCTTACTCGAGTAAGCATCTATTGATGTTCGCTTTTTG and the reverse primer: AATTCAAAAAGCGAACATCAATAGATGCTTACTCGAGTAAGCATCTATTGATGTTCGC. The primers were annealed and cloned into the plko.1 vector (Sigma, Rehovot Israel). The vector was transfected into cells using Lipofectamine 2000 (Invitrogen CA, USA). Thirty two hours after DNA transfection, cells were treated with the indicated medium for additional 16–18 hours, followed by Tf endocytosis protocol and icc with clathrin ab (BD Biosciences, CA, USA), or collected and processed for western blotting with clathrin ab (BD Biosciences, CA, USA). A second shRNA for clathrin heavy chain with the specific sequence TGAGCTGTTTGAAGAAGCA, total of 21 nucleotides at position 3387–3408 was kindly provided by Drs. Bacharach E. and Ehrlich M. (Tel Aviv University, Israel).

Quantitative Real-Time PCR

Total RNA was extracted from naive and αS over expressing MN9D cells treated with BSA +/−18:3 at 250 μM) using Tri Reagent (Sigma). RNA samples were treated with DNAase I (RNAase free) and reverse transcribed with random hexamers using Reverse-iT (ABgene Surrey, UK) to generate cDNA. Primers were generated according to (75) with 5′ primer sequence: 5-TCATGAGGGAAATCAATGATCGTA-3 and 3′ primer sequence 5-GCCCCAGAAGATATGTCGGAA-3. Results were normalized against the expression

levels of 18S. PCR analyses were performed using Applied biosystems Prism 7000 sequence detection system with CYBR Green Master Mix (Applied Biosystems).

FACS measurements of endocytosis and recycling

MN9D cells were plated 2 days before experiment and treated with the specified medium 16–18 hours before the labeling with AlexaFluor-488-Tf (invitrogen). For internalization, cells were conditioned in 25 μM 488-Tf at 37°C for the times indicated. Internalization was stopped by chilling the cells on ice. Access of 488-Tf was removed by 3 washes in ice-cold serum free medium and PBS. Surface bound Tf was removed by an acid wash with DMEM at pH 4.5 (pH adjusted with acetic acid) followed by neutralization with DMEM at pH 7.5 and a wash in PBS. Results are calculated relative to a sample treated in parallel (including acid wash) without incubation at 37°C (designated 0%) and relative to the sample with the highestinternalized transferrin in each test (100%). To measure recycling, cells were plated and treated with the specified medium as for internalization. Cells were then incubated for 1 hour at 37° in the presence of 25 μg/ml 488-Tf to completely label the receptor population. Unbound 488-Tf was removed by washes with pre-warmed serum-free medium (the amount of Tf at this point was referred as 100%). and the cells, now conditioned for indicated time at 37°C in serum free medium supplemented with BSA+/− 18:3 (50 and 250 μM respectively), 200 μg/ml deferoxamine and 600 μg/ml unlabeled human Tf. The release of 488-Tf was stopped by chilling the cells on ice. The fluorescence intensity of 488-Tf was measured for 10,000 cells by flow cytometry using an FACSCalibur (BD Biosciences, San Jose, CA) and the average intensity of the cell population was recorded for each time point.

Biotinylation of cell surface TfR

Surface levels of TfR were determined using the NHS-LC-biotin (Pierce Chemical Co., Rockford, IL) as previously described (76). Briefly, cells were plated in 60 mm dishes two days before the biotinylation and treated with the specified medium for 16–18 hours before cooling by three quick washes with ice-cold PBS containing Ca^{2+} and Mg^{2+} (PBS++). Selective biotinylation of the cell surface proteins was performed at 4°C with two rounds of 20 min incubations of 0.5 mg/ml NHS-LC-biotin in 10mM Boric Acid and 150mM NaCl pH 8.0. Cells were washed and free sulfhydryl groups were quenched for 15 min at 4°C with 50 mM Glycine in PBS++. Whole cell lysate was prepared in 0.5 ml Triton lysis Buffer [100 mM NaCl, 5mM EDTA, pH 8.0, 100mM triethanolamine Cl, pH 8.6, 2.5% (v/v) Triton X-100, 0.02% (v/v) sodium azide and Protein inhibitor cocktail 1:100 (Sigma)]. Cells were scraped and vortex at 4°C for 20 min. Cell lysate was centrifuged for 30 minutes at 12,000g at 4°C. Supernatant was transferred to a fresh tube. Protein concentration was determined using BCA kit (Pierce). Aliquots of equal protein concentration (30 μg) were analyzed by western blotting for total TfR, aliquots of 45 μg protein were used to immuno-percipitate TfR on streptavidine agarose beads (sigma S1638).

Primary neuronal culture

Hippocampal cell cultures were prepared as described previously (Vardinon-Friedman et al., 2000). Briefly, hippocampal CA1-CA3 regions were dissected from 1- to 2-d-old C57BL/6 mice, dissociated by trypsin treatment, followed by triturationwith a siliconized Pasteur pipette, and then plated onto coverslipscoated with poly-D-lysine (Sigma, St. Louis, MO) inside 24 well dish. Culture medium consisted of MEM (Invitrogen, San Diego, CA), 0.6% glucose, 0.1 gm/l bovine Tf (Calbiochem, La Jolla, CA), 0.25 gm/l insulin (Sigma), 0.3 gm/l glutamine, 5–10% fetal calf serum (Sigma), 2% B-27 supplement (Invitrogen). To eliminate the glia cells, 8μM cytosine *b*-D-arabinofuranoside (Sigma) were added to the culture 3 days after preparation and removed after additional 3–4 days. Cultures were maintained at 37°Cin a 95% air/5% CO_2 humidified incubator, and culture medium was replaced every 4–7 d. Experiments were performed on cultures grown for 18 days. Normal mice are C57BL/6

obtained from Jackson laboratories (Maine USA) and αS −/− mice are C57BL/6 obtained from Harlan (Rehovot, Israel) (74).

FM1-43 internalization into synaptic vesicles

Neurons were loaded with 10 μM FM1-43 by high K^+ application or without chemical stimulation. Specifically, neurons were chemically induced in solution containing 90mM K^+ in buffer containing: NaCl, 31.5 mM; KCl, 2 mM; $CaCl_2$ mM, 2; $MgCl_2$, 2 mM; Hepes, 30 mM; glucose, 10mM buffered to pH 7.4 for 60 s or maintained in PBS (calcium and magnesium free) in the presence of FM1-43. Neurons were than washed (2–3 times) in low KCl solution containing: 119 mM NaCl; 2.5 mM KCl, 2 mM $CaCl_2$, 2 mM $MgCl_2$, 25 mM Hepes, 30mM glucose, buffered to pH 7.4 for 5 min. A second stimulation with 90 mM KCl solution without FM1-43 for 60 s was applied for destaining, followed by washes and fixing the neurons in 4% PFA. Neurons were than processed for icc with anti synaptophysin ab (DAKO cytomation Glostrup, Denmark) as described above.

Imaging and quantitative analysis of endocytosis

Most experiments were documented with a zeiss LSM 410 confocal laser scanning system. The system is equipped with an argon laser 488 excitation with 510 nm pass-barrier filter and two helium-neon lasers, excitation at 543 nm (570 nm emission) and excitation at 643 nm (665 nm emission). Fluorescence was collected simultaneously with DIC images according to Nomarski using a transmitted light detector. The fluorescence was collected by employing a 63X1.4 planApochromate oil immersion lens (Zeiss). In each experiment, exciting laser, intensity, background levels, PMT gain, contrast and electronic zoom size were maintained at the same level. Alternatively, we used (As indicated) an Olympus confocal laser scanning system FluView FV300 equipped with an UPlanSApo 60X/1.35 (oil) lens. Lasers: Melles Griot 488 Ion Argon laser and 633 He/Ne laser.

Image series were analyzed with Pro/Image J softwares (Media Cybernetics Inc. MD, USA). The FM1-43 heavily labeled endosomes increased the probability that multiple endosomes would be clustered into an individual fluorescent point. Therefore, for the majority of experiments (FM1 43/Alexa488 Tf/Cy5-clathrin and synaptophysin figures 2,3,4,7 and 8) endocytosis was measured as the sum of fluorescent signal above threshold divided by the area of the cell. Fluorescence intensity in a single cell was obtained by choosing the image plane with the greatest number of stained endosomes, measuring the average fluorescence intensity across the entire cell area, and subtracting the nonspecific background fluorescence. Background was subtracted using imageJ rolling ball algorithm, (*Rolling Ball Radius* =50). The presented values are average integrated density of 5–20 cells. For Tf Dose response experiment (Fig 4) - A computer-controlled microscope stage was used for acquiring vertical series of images through the entire depth of a cell at 1 μm increments. The projections were analyzed using “particle analysis” (to define the vesicle we used limitation in size of 10 pixels and above and circularity of 0–1 of imageJ definitions). The values represented are average properties of all labeled vesicles of 6 different cells for each treatment. Image acquisition parameters were kept fixed for each experiment. All intensity values are presented in arbitrary units.

Acknowledgments

This work was supported by the National Institute of Neurological Disorders and Stroke (NINDS) R01 NS051318 (D.J.S. and R.S.).

Abbreviations

αS	α-Synuclein
PD	Parkinson's Disease
FA	Fatty acids
PUFA	Polyunsaturated fatty acids
MUFA	Monounsaturated fatty acids
SFA	Saturated fatty acids
CME	Clathrin mediated endocytosis
RME	Receptor mediated endocytosis
Tf	Transferrin
TfR	Transferrin Receptor

References

1. Ibanez P, Bonnet AM, Debarges B, Lohmann E, Tison F, Pollak P, Agid Y, Durr A, Brice A. Causal relation between alpha-synuclein gene duplication and familial Parkinson's disease. Lancet. 2004; 364(9440):1169–1171. [PubMed: 15451225]
2. Singleton AB, Farrer M, Johnson J, Singleton A, Hague S, Kachergus J, Hulihan M, Peuralinna T, Dutra A, Nussbaum R, Lincoln S, Crawley A, Hanson M, Maraganore D, Adler C, et al. alpha-Synuclein locus triplication causes Parkinson's disease. Science. 2003; 302(5646):841. [PubMed: 14593171]
3. Baba M, Nakajo S, Tu PH, Tomita T, Nakaya K, Lee VM, Trojanowski JQ, Iwatsubo T. Aggregation of alpha-synuclein in Lewy bodies of sporadic Parkinson's disease and dementia with Lewy bodies. Am J Pathol. 1998; 152(4):879–884. [PubMed: 9546347]
4. Spillantini MG, Schmidt ML, Lee VM, Trojanowski JQ, Jakes R, Goedert M. Alpha-synuclein in Lewy bodies. Nature. 1997; 388(6645):839–840. [PubMed: 9278044]
5. Choi W, Zibaee S, Jakes R, Serpell LC, Davletov B, Crowther RA, Goedert M. Mutation E46K increases phospholipid binding and assembly into filaments of human alpha-synuclein. FEBS Lett. 2004; 576(3):363–368. [PubMed: 15498564]
6. Kruger R, Kuhn W, Muller T, Woitalla D, Graeber M, Kosel S, Przuntek H, Epplen JT, Schols L, Riess O. Ala30Pro mutation in the gene encoding alpha-synuclein in Parkinson's disease. Nat Genet. 1998; 18(2):106–108. [PubMed: 9462735]
7. Polymeropoulos MH, Lavedan C, Leroy E, Ide SE, Dehejia A, Dutra A, Pike B, Root H, Rubenstein J, Boyer R, Stenroos ES, Chandrasekharappa S, Athanassiadou A, Papapetropoulos T, Johnson WG, et al. Mutation in the alpha-synuclein gene identified in families with Parkinson's disease. Science. 1997; 276(5321):2045–2047. [PubMed: 9197268]
8. Bussell R Jr, Ramlall TF, Eliezer D. Helix periodicity, topology, and dynamics of membrane-associated alpha-synuclein. Protein Sci. 2005; 14(4):862–872. [PubMed: 15741347]
9. Davidson WS, Jonas A, Clayton DF, George JM. Stabilization of alpha-synuclein secondary structure upon binding to synthetic membranes. J Biol Chem. 1998; 273(16):9443–9449. [PubMed: 9545270]
10. Perrin RJ, Woods WS, Clayton DF, George JM. Exposure to long chain polyunsaturated fatty acids triggers rapid multimerization of synucleins. J Biol Chem. 2001; 276(45):41958–41962. [PubMed: 11553616]
11. Perrin RJ, Woods WS, Clayton DF, George JM. Interaction of human alpha-Synuclein and Parkinson's disease variants with phospholipids. Structural analysis using site-directed mutagenesis. J Biol Chem. 2000; 275(44):34393–34398. [PubMed: 10952980]
12. Ulmer TS, Bax A, Cole NB, Nussbaum RL. Structure and dynamics of micelle-bound human alpha-synuclein. J Biol Chem. 2005; 280(10):9595–9603. [PubMed: 15615727]

13. Zhu M, Li J, Fink AL. The association of alpha-synuclein with membranes affects bilayer structure, stability, and fibril formation. J Biol Chem. 2003; 278(41):40186–40197. [PubMed: 12885775]

14. Zhu M, Fink AL. Lipid binding inhibits alpha-synuclein fibril formation. J Biol Chem. 2003; 278(19):16873–16877. [PubMed: 12621030]

15. Chandra S, Chen X, Rizo J, Jahn R, Sudhof TC. A broken alpha-helix in folded alpha-Synuclein. J Biol Chem. 2003; 278(17):15313–15318. [PubMed: 12586824]

16. Lucke C, Gantz DL, Klimtchuk E, Hamilton JA. Interactions between fatty acids and alpha-synuclein. J Lipid Res. 2006; 47(8):1714–1724. [PubMed: 16687662]

17. George JM, Jin H, Woods WS, Clayton DF. Characterization of a novel protein regulated during the critical period for song learning in the zebra finch. Neuron. 1995; 15(2):361–372. [PubMed: 7646890]

18. Sharon R, Goldberg MS, Bar-Josef I, Betensky RA, Shen J, Selkoe DJ. alpha-Synuclein occurs in lipid-rich high molecular weight complexes, binds fatty acids, and shows homology to the fatty acid-binding proteins. Proc Natl Acad Sci U S A. 2001; 98(16):9110–9115. [PubMed: 11481478]

19. Fortin DL, Troyer MD, Nakamura K, Kubo S, Anthony MD, Edwards RH. Lipid rafts mediate the synaptic localization of alpha-synuclein. J Neurosci. 2004; 24(30):6715–6723. [PubMed: 15282274]

20. Cole NB, Murphy DD, Grider T, Rueter S, Brasaemle D, Nussbaum RL. Lipid droplet binding and oligomerization properties of the Parkinson's disease protein alpha-synuclein. J Biol Chem. 2002; 277(8):6344–6352. [PubMed: 11744721]

21. Jensen PH, Nielsen MS, Jakes R, Dotti CG, Goedert M. Binding of alpha-synuclein to brain vesicles is abolished by familial Parkinson's disease mutation. J Biol Chem. 1998; 273(41):26292–26294. [PubMed: 9756856]

22. McLean PJ, Kawamata H, Ribich S, Hyman BT. Membrane association and protein conformation of alpha-synuclein in intact neurons. Effect of Parkinson's disease-linked mutations. J Biol Chem. 2000; 275(12):8812–8816. [PubMed: 10722726]

23. Clayton DF, George JM. Synucleins in synaptic plasticity and neurodegenerative disorders. J Neurosci Res. 1999; 58(1):120–129. [PubMed: 10491577]

24. Clayton DF, George JM. The synucleins: a family of proteins involved in synaptic function, plasticity, neurodegeneration and disease. Trends Neurosci. 1998; 21(6):249–254. [PubMed: 9641537]

25. Sharon R, Bar-Joseph I, Mirick GE, Serhan CN, Selkoe DJ. Altered fatty acid composition of dopaminergic neurons expressing alpha-synuclein and human brains with alpha-synucleinopathies. J Biol Chem. 2003; 278(50):49874–49881. [PubMed: 14507911]

26. Golovko MY, Rosenberger TA, Faergeman NJ, Feddersen S, Cole NB, Pribill I, Berger J, Nussbaum RL, Murphy EJ. Acyl-CoA synthetase activity links wild-type but not mutant alpha-synuclein to brain arachidonate metabolism. Biochemistry. 2006; 45(22):6956–6966. [PubMed: 16734431]

27. Golovko MY, Faergeman NJ, Cole NB, Castagnet PI, Nussbaum RL, Murphy EJ. alpha-Synuclein Gene Deletion Decreases Brain Palmitate Uptake and Alters the Palmitate Metabolism in the Absence of alpha-Synuclein Palmitate Binding. Biochemistry. 2005; 44(23):8251–8259. [PubMed: 15938614]

28. Castagnet PI, Golovko MY, Barcelo-Coblijn GC, Nussbaum RL, Murphy EJ. Fatty acid incorporation is decreased in astrocytes cultured from alpha-synuclein gene-ablated mice. J Neurochem. 2005; 94(3):839–849. [PubMed: 16033426]

29. Barcelo-Coblijn G, Golovko MY, Weinhofer I, Berger J, Murphy EJ. Brain neutral lipids mass is increased in alpha-synuclein gene-ablated mice. J Neurochem. 2007; 101(1):132–141. [PubMed: 17250686]

30. Golovko MY, Rosenberger TA, Feddersen S, Faergeman NJ, Murphy EJ. alpha-Synuclein gene ablation increases docosahexaenoic acid incorporation and turnover in brain phospholipids. J Neurochem. 2007

31. Barcelo-Coblijn G, Golovko MY, Weinhofer I, Berger J, Murphy EJ. Brain neutral lipids mass is increased in alpha-synuclein gene-ablated mice. J Neurochem. 2007

32. Kirchhausen T, Boll W, van Oijen A, Ehrlich M. Single-molecule live-cell imaging of clathrin-based endocytosis. Biochem Soc Symp. 2005; 72(71):76.
33. Le Roy C, Wrana JL. Signaling and endocytosis: a team effort for cell migration. Dev Cell. 2005; 9(2):167–168. [PubMed: 16054022]
34. Conner SD, Schmid SL. Regulated portals of entry into the cell. Nature. 2003; 422(6927):37–44. [PubMed: 12621426]
35. Galli T, Haucke V. Cycling of synaptic vesicles: how far? How fast! Sci STKE. 2004; 2004(264):re19. [PubMed: 15613688]
36. Murthy VN, De Camilli P. Cell biology of the presynaptic terminal. Annu Rev Neurosci. 2003; 26:701–728. [PubMed: 14527272]
37. Marza E, Lesa GM. Polyunsaturated fatty acids and neurotransmission in Caenorhabditis elegans. Biochem Soc Trans. 2006; 34(Pt 1):77–80. [PubMed: 16417487]
38. Darios F, Davletov B. Omega-3 and omega-6 fatty acids stimulate cell membrane expansion by acting on syntaxin 3. Nature. 2006; 440(7085):813–817. [PubMed: 16598260]
39. Delion S, Chalon S, Herault J, Guilloteau D, Besnard JC, Durand G. Chronic dietary alpha linoleic acid deficiency alters dopaminergic and serotoninergic neurotransmission in rats. J Nutr. 1994; 124:2466–2476. [PubMed: 16856329]
40. Delion S, Chalon S, Guilloteau D, Lejeune B, Besnard JC, Durand G. Age-related changes in phospholipid fatty acid composition and monoaminergic neurotransmission in the hippocampus of rats fed a balanced or an n-3 polyunsaturated fatty acid-deficient diet. J Lipid Res. 1997; 38(4): 680–689. [PubMed: 9144083]
41. de la Presa-Owens S, Innis SM, Rioux FM. Addition of triglycerides with arachidonic acid or docosahexaenoic acid to infant formula has tissue- and lipid class-specific effects on fatty acids and hepatic desaturase activities in formula-fed piglets. J Nutr. 1998; 128(8):1376–1384. [PubMed: 9687559]
42. Zimmer L, Delpal S, Guilloteau D, Aioun J, Durand G, Chalon S. Chronic n-3 polyunsaturated fatty acid deficiency alters dopamine vesicle density in the rat frontal cortex. Neurosci Lett. 2000; 284(1–2):25–28. [PubMed: 10771153]
43. Zimmer L, Durand G, Guilloteau D, Chalon S. n-3 polyunsaturated fatty acid deficiency and dopamine metabolism in the rat frontal cortex. Lipids. 1999; 34 (Suppl):S251. [PubMed: 10419169]
44. Chalon S, Delion-Vancassel S, Belzung C, Guilloteau D, Leguisquet AM, Besnard JC, Durand G. Dietary fish oil affects monoaminergic neurotransmission and behavior in rats. J Nutr. 1998; 128(12):2512–2519. [PubMed: 9868201]
45. Chernomordik LV, Leikina E, Frolov V, Bronk P, Zimmerberg J. An early stage of membrane fusion mediated by the low pH conformation of influenza hemagglutinin depends upon membrane lipids. J Cell Biol. 1997; 136(1):81–93. [PubMed: 9008705]
46. Chernomordik LV, Leikina E, Kozlov MM, Frolov VA, Zimmerberg J. Structural intermediates in influenza haemagglutinin-mediated fusion. Mol Membr Biol. 1999; 16(1):33–42. [PubMed: 10332735]
47. Cabin DE, Shimazu K, Murphy D, Cole NB, Gottschalk W, McIlwain KL, Orrison B, Chen A, Ellis CE, Paylor R, Lu B, Nussbaum RL. Synaptic vesicle depletion correlates with attenuated synaptic responses to prolonged repetitive stimulation in mice lacking alpha-synuclein. J Neurosci. 2002; 22(20):8797–8807. [PubMed: 12388586]
48. Murphy DD, Rueter SM, Trojanowski JQ, Lee VM. Synucleins are developmentally expressed, and alpha-synuclein regulates the size of the presynaptic vesicular pool in primary hippocampal neurons. J Neurosci. 2000; 20(9):3214–3220. [PubMed: 10777786]
49. Sharon R, Bar-Joseph I, Frosch MP, Walsh DM, Hamilton JA, Selkoe DJ. The formation of highly soluble oligomers of alpha-synuclein is regulated by fatty acids and enhanced in Parkinson's disease. Neuron. 2003; 37(4):583–595. [PubMed: 12597857]
50. Betz WJ, Mao F, Smith CB. Imaging exocytosis and endocytosis. Curr Opin Neurobiol. 1996; 6(3):365–371. [PubMed: 8794083]
51. Ryan TA. Presynaptic imaging techniques. Curr Opin Neurobiol. 2001; 11(5):544–549. [PubMed: 11595486]

52. McNamara RK, Carlson SE. Role of omega-3 fatty acids in brain development and function: potential implications for the pathogenesis and prevention of psychopathology. Prostaglandins Leukot Essent Fatty Acids. 2006; 75(4–5):329–349. [PubMed: 16949263]
53. Hinrichsen L, Harborth J, Andrees L, Weber K, Ungewickell EJ. Effect of clathrin heavy chain- and alpha-adaptin-specific small inhibitory RNAs on endocytic accessory proteins and receptor trafficking in HeLa cells. J Biol Chem. 2003; 278(46):45160–45170. [PubMed: 12960147]
54. Cochilla AJ, Angleson JK, Betz WJ. Monitoring secretory membrane with FM1-43 fluorescence. Annu Rev Neurosci. 1999; 22:1–10. [PubMed: 10202529]
55. Betz WJ, Bewick GS. Optical analysis of synaptic vesicle recycling at the frog neuromuscular junction. Science. 1992; 255(5041):200–203. [PubMed: 1553547]
56. Ryan TA. A pre-synaptic to-do list for coupling exocytosis to endocytosis. Curr Opin Cell Biol. 2006; 18(4):416–421. [PubMed: 16806881]
57. Jakes R, Spillantini MG, Goedert M. Identification of two distinct synucleins from human brain. FEBS Lett. 1994; 345(1):27–32. [PubMed: 8194594]
58. Iwai A, Masliah E, Yoshimoto M, Ge N, Flanagan L, De Silva R, Kittel ATS. The precursor protein of non Ab component of Alzheimers disease amyloid is a presynaptic protein of the central nervous system. Neuron. 1995; 14:467–475. [PubMed: 7857654]
59. Maroteaux L, Campanelli JT, Scheller RH. Synuclein: a neuron-specific protein localized to the nucleus and presynaptic nerve terminal. J Neurosci. 1988; 8(8):2804–2815. [PubMed: 3411354]
60. Larsen KE, Schmitz Y, Troyer MD, Mosharov E, Dietrich P, Quazi AZ, Savalle M, Nemani V, Chaudhry FA, Edwards RH, Stefanis L, Sulzer D. {alpha}-Synuclein Overexpression in PC12 and Chromaffin Cells Impairs Catecholamine Release by Interfering with a Late Step in Exocytosis. J Neurosci. 2006; 26(46):11915–11922. [PubMed: 17108165]
61. Chandra S, Fornai F, Kwon HB, Yazdani U, Atasoy D, Liu X, Hammer RE, Battaglia G, German DC, Castillo PE, Sudhof TC. Double-knockout mice for alpha- and beta-synucleins: effect on synaptic functions. Proc Natl Acad Sci U S A. 2004; 101(41):14966–14971. [PubMed: 15465911]
62. Abeliovich A, Schmitz Y, Farinas I, Choi-Lundberg D, Ho WH, Castillo PE, Shinsky N, Verdugo JM, Armanini M, Ryan A, Hynes M, Phillips H, Sulzer D, Rosenthal A. Mice lacking alpha-synuclein display functional deficits in the nigrostriatal dopamine system. Neuron. 2000; 25(1): 239–252. [PubMed: 10707987]
63. Cooper AA, Gitler AD, Cashikar A, Haynes CM, Hill KJ, Bhullar B, Liu K, Xu K, Strathearn KE, Liu F, Cao S, Caldwell KA, Caldwell GA, Marsischky G, Kolodner RD, et al. Alpha-synuclein blocks ER-Golgi traffic and Rab1 rescues neuron loss in Parkinson's models. Science. 2006; 313(5785):324–328. [PubMed: 16794039]
64. Gitler AD, Bevis BJ, Shorter J, Strathearn KE, Hamamichi S, Su LJ, Caldwell KA, Caldwell GA, Rochet JC, McCaffery JM, Barlowe C, Lindquist S. The Parkinson's disease protein alpha-synuclein disrupts cellular Rab homeostasis. Proc Natl Acad Sci U S A. 2008; 105(1):145–150. [PubMed: 18162536]
65. Chandra S, Gallardo G, Fernandez-Chacon R, Schluter OM, Sudhof TC. Alpha-synuclein cooperates with CSPalpha in preventing neurodegeneration. Cell. 2005; 123(3):383–396. [PubMed: 16269331]
66. Ungar D, Hughson FM. SNARE protein structure and function. Annu Rev Cell Dev Biol. 2003; 19:493–517. [PubMed: 14570579]
67. Sudhof TC. The synaptic vesicle cycle. Annu Rev Neurosci. 2004; 27:509–547. [PubMed: 15217342]
68. Fernandez-Alfonso T, Ryan TA. The efficiency of the synaptic vesicle cycle at central nervous system synapses. Trends Cell Biol. 2006; 16(8):413–420. [PubMed: 16839766]
69. Chen X, de Silva HA, Pettenati MJ, Rao PN, St George-Hyslop P, Roses AD, Xia Y, Horsburgh K, Ueda K, Saitoh T. The human NACP/alpha-synuclein gene: chromosome assignment to 4q21.3-q22 and TaqI RFLP analysis. Genomics. 1995; 26(2):425–427. [PubMed: 7601479]
70. Haucke V. Phosphoinositide regulation of clathrin-mediated endocytosis. Biochem Soc Trans. 2005; 33(Pt 6):1285–1289. [PubMed: 16246100]

71. Crawford GD Jr, Le WD, Smith RG, Xie WJ, Stefani E, Appel SH. A novel N18TG2 x mesencephalon cell hybrid expresses properties that suggest a dopaminergic cell line of substantia nigra origin. J Neurosci. 1992; 12(9):3392–3398. [PubMed: 1356145]

72. Choi HK, Won LA, Kontur PJ, Hammond DN, Fox AP, Wainer BH, Hoffmann PC, Heller A. Immortalization of embryonic mesencephalic dopaminergic neurons by somatic cell fusion. Brain Res. 1991; 552(1):67–76. [PubMed: 1913182]

73. Giasson BI, Duda JE, Quinn SM, Zhang B, Trojanowski JQ, Lee VM. Neuronal alpha-synucleinopathy with severe movement disorder in mice expressing A53T human alpha-synuclein. Neuron. 2002; 34(4):521–533. [PubMed: 12062037]

74. Specht CG, Schoepfer R. Deletion of the alpha-synuclein locus in a subpopulation of C57BL/6J inbred mice. BMC Neurosci. 2001; 2(1):11. [PubMed: 11591219]

75. Dupic F, Fruchon S, Bensaid M, Loreal O, Brissot P, Borot N, Roth MP, Coppin H. Duodenal mRNA expression of iron related genes in response to iron loading and iron deficiency in four strains of mice. Gut. 2002; 51(5):648–653. [PubMed: 12377801]

76. Aroeti B, Kosen PA, Kuntz ID, Cohen FE, Mostov KE. Mutational and secondary structural analysis of the basolateral sorting signal of the polymeric immunoglobulin receptor. J Cell Biol. 1993; 123(5):1149–1160. [PubMed: 8245123]

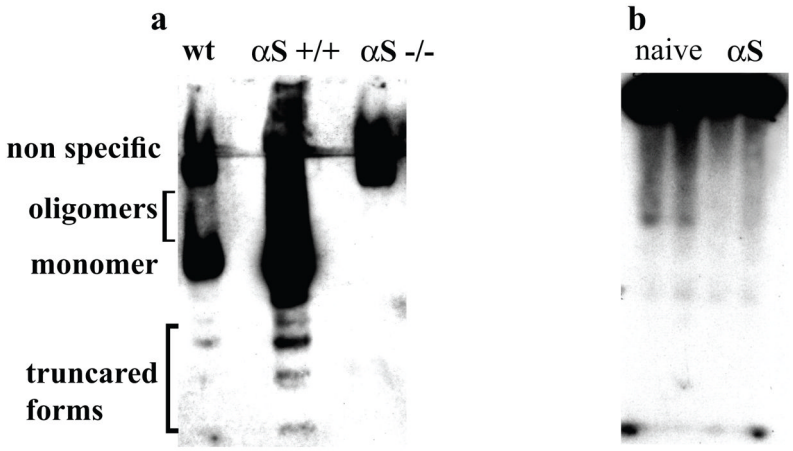

Figure 1. αS occurs in soluble oligomers in vivo and promote incorporation of 14C OA

(a) Samples of post 100,000g cytosols (15μg) of brains from wt (16 month), αS +/+ (9 month) and αS −/− (15 month) mice were incubated with Lipidex-1000 at 4 °C for 16 hours followed by native gel electrophoresis (10% Tris-Glycine) and western blotting with syn-1 antibody. (b) Samples of post 100,000g cytosols (15 μg) from naive or αS-overexpressing MES cells conditioned with ^{14}C OA (35 μM) for 16 hours and subjected to native gel electrophoresis (autoradiogram).

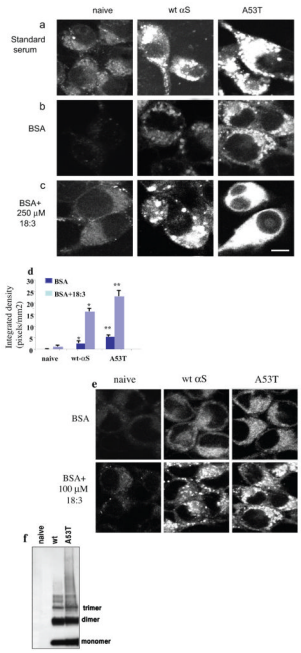

Figure 2. FM1-43 internalization into MES 23.5 dopaminergic cells is induced by αS over expression and 18:3 PUFA

(a). Naive, wt and A53T αS over expressing MES cells conditioned in standard serum-containing medium and labeled with 2.5 μM FM1-43 fluorescent dye (molecular probes Eugene, OR) for 4 minutes. Access of dye was removed, and 10 minutes later the cells were fixed and tested for intracellular FM1-43 fluorescence. Pictures were taken in confocal, laser scanning microscope (Zeiss LSM 410) under non-saturating conditions. (b). Naïve, wt and A53T αS over expressing MES cells were conditioned for 16–18 hours in serum-free medium supplemented with 50μM BSA, followed by labeling with FM1-43 as in (a). (c). Cells as in (b) but conditioned in serum free medium supplemented with BSA only (50 μM) plus 250 μM 18:3 PUFA. (d). Quantitative presentation of the intracellular FM1-43 in BSA vs. PUFA treated cultures. Quantitation was performed on the captured images at selected image plane with the greatest intracellular FM1-43 signal, using ImageJ software, measuring the average fluorescence intensity (above threshold) across the entire cell divided by the area of the tested cell. Mean of 10–15 cells ± SD. * significant over the corresponding treatment in naïve cells and ** significant over the corresponding treatment in wt αS over expressing cells. TTEST P value < 0.05 (e) Cells were treated as in (b) and (c) but with 20 μM BSA with or without 100 μM 18:3 respectively. (f) Western blot of cytosolic extract from naïve, wt and A53T over expressing cells, treated for oligomers detection (49) and probed with anti αS H3C ab. Bar represents 10 μm.

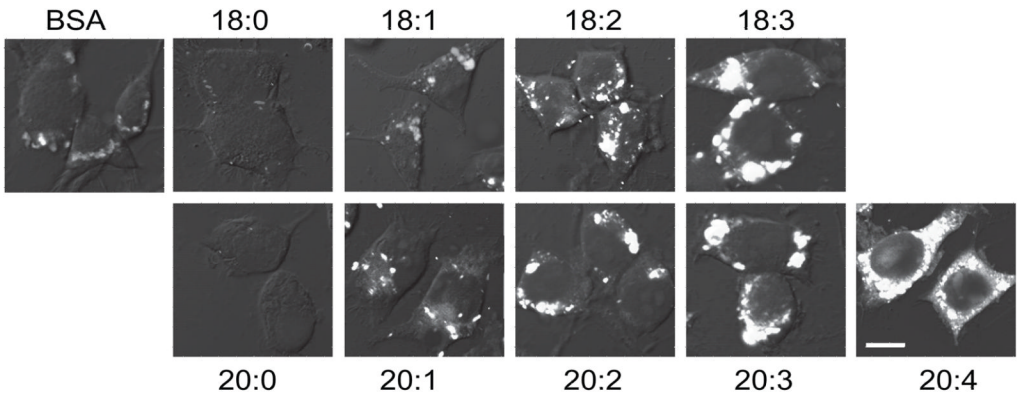

Figure 3. FM1-43 endocytosis as a function of fatty acid length and saturation

αS over expressing MES dopaminergic cells were grown on 12-wells cover glass and conditioned for 16 hours in serum free medium supplemented with BSA only (50 μM) or with 250 μM of the indicated FA in sister cultures, in parallel. Cells were then labeled with FM1-43 as in Fig 2a and fixed. Representative pictures are presented. Image acquisition by Zeiss LSM 410. Acquisition parameters were kept fixed throughout. Bar represents 10 μm.

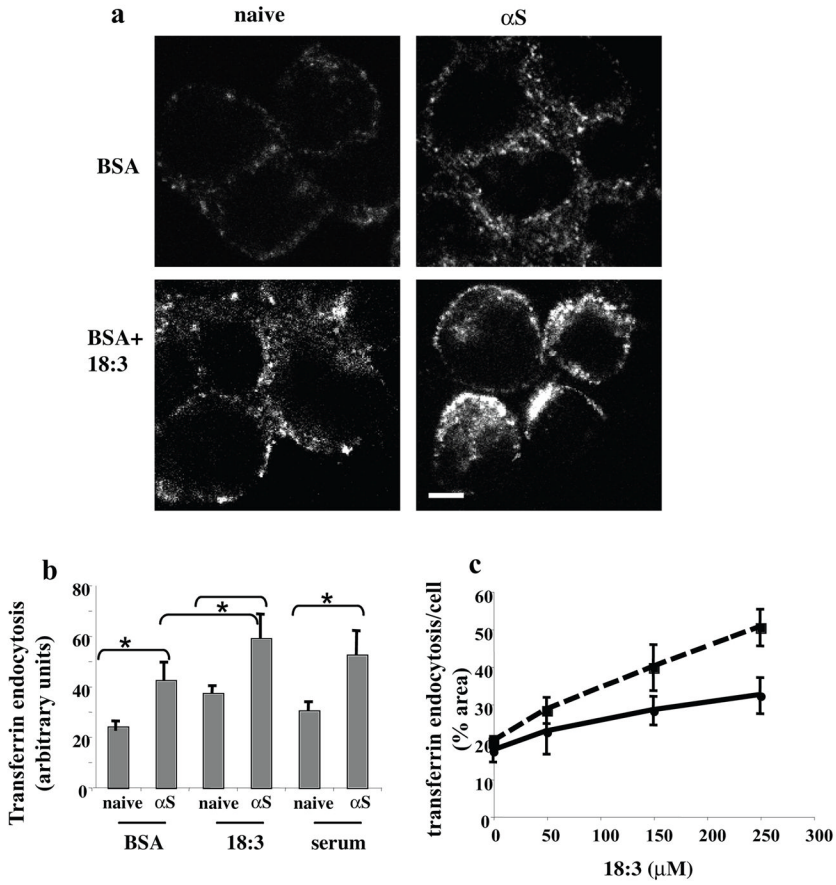

Figure 4. αS and PUFA act to induce endocytosis of Tf

(a) Naïve and wt αS over expressing MN9D cells were grown on 12-wells cover glass and conditioned for 18 hours in DMEM containing 250 μM 18:3 PUFA or DMEM with BSA (50 μM). Alexa-488 human Tf (molecular probes, Eugene, Or) (50μg/ml) were then added to the cells in plain DMEM medium (without serum, antibiotics or nutrients) in cold, to allow binding of Tf to the TfR. After the removal of unbound Tf, cells were incubated for 10 minutes at 37° in serum free medium supplemented with BSA or PUFA accordingly. Cells were then fixed and observed by Olympus FluoView FV300 confocal microscope. (b) Quantitation of Alexa-488 Tf endocytosis. Cells and treatments as in (a) plus naïve and αS over expressing MN9D conditioned in standard serum-supplemented medium. All images were taken at the same settings and the image plane containing maximal intracellular signal was selected. Threshold was set as to measure only endocytic vesicles, rather then including a more diffuse background. All measurements were of "selected region of interest" normalized to cell area. Mean of n=10 cells of each treatment ± SD. *, ttest $p<0.01$. (c) the endocytosis of Alexa-488-Tf is PUFA- dose dependent in naïve and αS over expressing cells. αS over expressing SK-N-SH cells were grown as in (a), conditioned with the indicated 18:3 concentration and quantified as in (b). Graph presenting the sum of signal in endocytic vesicles (above threshold) to 18:3 concentrations. n=10 cells counted ± SD of αS over expressing cells (Dashed line) and naive (filled line). Bar represents 10 μm.

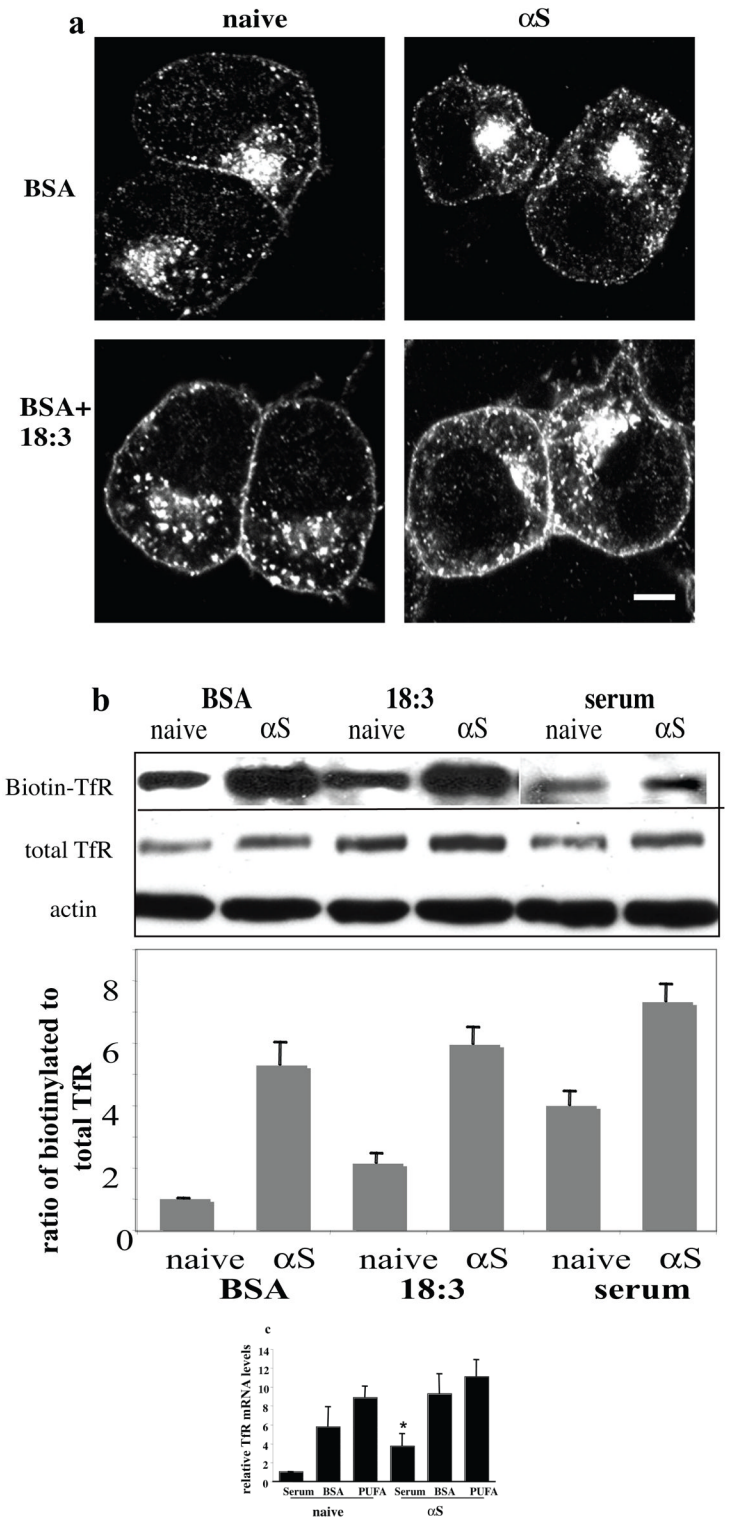

Figure 5. αS and PUFA affect TfR levels and cellular distribution

(a) Naïve and human wt αS over expressing MN9D neuronal cells were grown on 12-wells cover glass, conditioned for 18 hours in 250 μM 18:3 PUFA or in BSA only (50 μM). Tf (50μM) was added as in fig. 4a and cells were processed for icc using anti TfR ab (Zymed

Laboratories CA, USA). (b) αS and PUFA increase levels of cell surface TfR. Biotinylation of cell surface TfR, normalized to total TfR using anti TfR ab (Zymed Laboratories CA, USA) and to actin (Sigma Rehovot Israel), and its densiometric analysis. (c) αS and PUFA induce TfR expression levels. Quantitative Real Time PCR reaction of total RNA extracted from naïve and αS over expressing MN9D cells treated in BSA +/− 18:3 (at 50 and 250 μM for BSA and 18:3). The levels of TfR mRNA was normalized to the 18S mRNA. Mean of three experiments ± SE. Bar represents 10 μm.

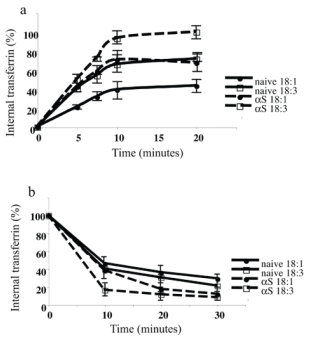

Figure 6. αS and PUFA activate the rate of membrane trafficking

Naïve and wt αS over expressing MN9D cells were conditioned for 16–18 hours in serum-free medium supplemented with BSA+/− 18:3 PUFA (50 and 250 μM for BSA and PUFA respectively). TfRs were loaded with Alexa 488 Tf. Recycling of Tf was measured by FACS analyses (see methods). Graphs present the mean and SD of three experiments. (a) internalization, results are presented as percent of the sample with maximal internalized transferrin in each test. (b) recycling, results are presented as the loss (percent) of cell associated fluorescence for each treatment.

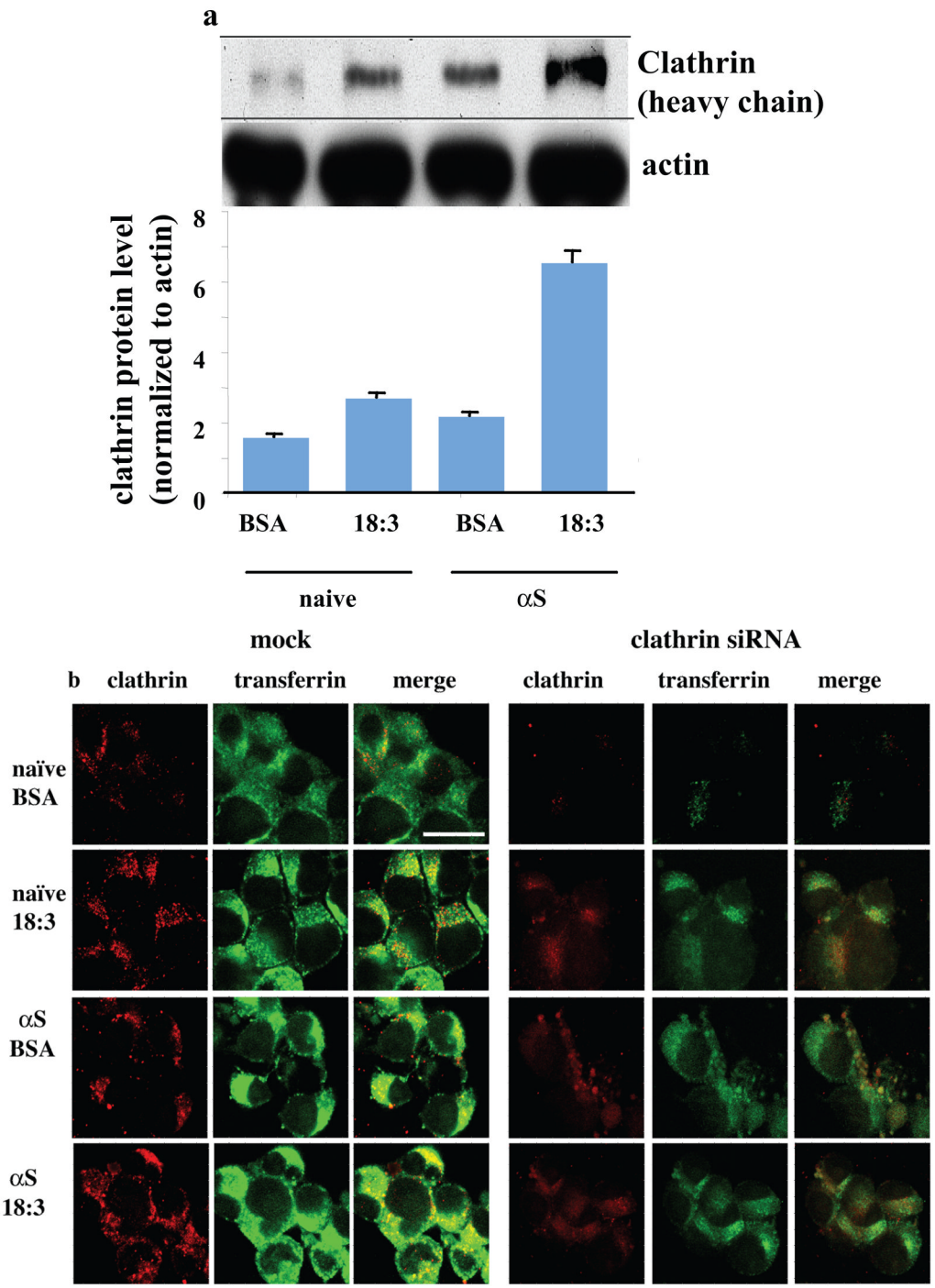

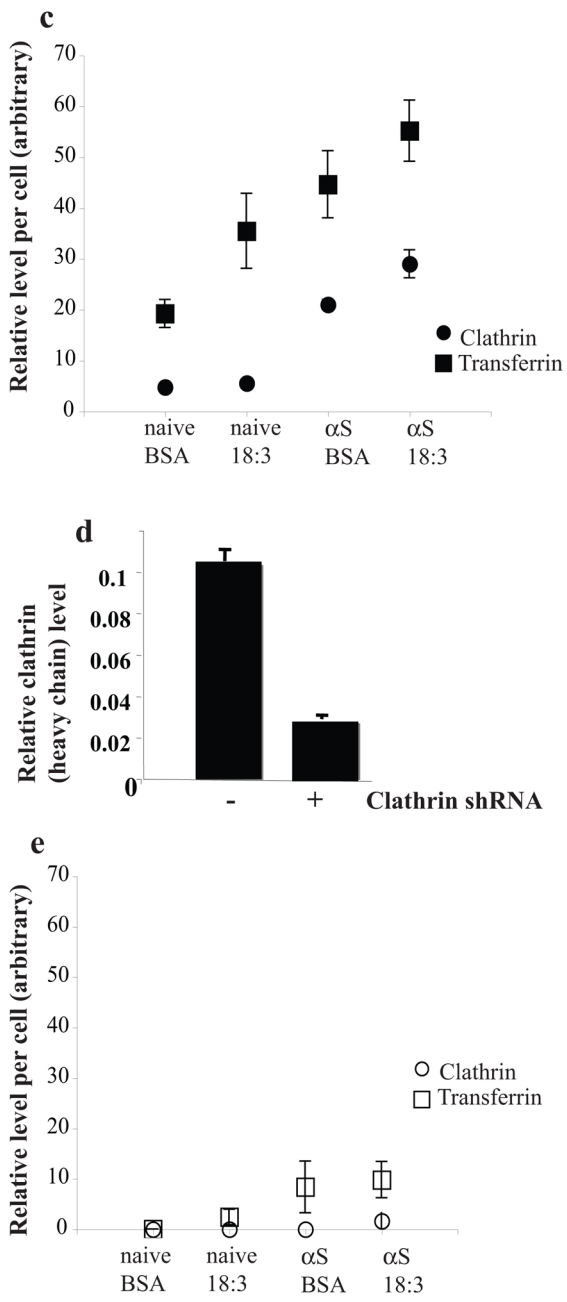

Figure 7. αS and PUFA -induced Tf endocytosis is clathrin dependent

Naïve and wt αS over expressing MES cells were conditioned for 16–18 hours in serum-free medium supplemented with BSA+/− 18:3 PUFA (50 and 250 μM for BSA and PUFA respectively). Whole cell extract was analyzed by western blot and probed with clathrin (heavy chain) antibody. Results are normalized to actin and presented in arbitrary units. (b) Naïve and wt αS over expressing MN9D cells were grown on 12-wells cover glass and transfected with either mock (empty Plko.1 plasmid) - or shRNA for clathrin heavy chain. Thirty two hours post DNA transfection the cells were transferred to serum-free conditioning medium, supplemented with BSA+18:3 PUFA (50 and 250 μM for BSA and FA respectively) for 16 hr. 48 hr post DNA-transfection, 50μg/ml Alexa-488 human Tf were added to the cells (as in Fig 4a). Cells were fixed and processed for detection of Alexa 488-

Tf and icc with anti clathrin antibody (see methods). (c) Quantitation of Alexa-488 Tf endocytosis and clathrin protein levels. Cells and treatments as in (b), images were taken at the same settings and the image plane containing maximal intracellular signal was selected. Threshold was set as to measure only endocytic vesicles, rather then including a more diffuse background. All measurements were of "selected region of interest" normalized to cell area. Mean of n=10 cells of each treatment ± SD. ANOVA $p<0.001$. (d) Clathrin (heavy chain) protein levels in αS over expressing MES cells transfected with plko.1 or clathrin shRNA and treated with PUFA as in (b). Deniomentic analyses of western blot probed with anti clathrin antibody and normalized to tubulin signal on the same blot. (e) Quantitation of Alexa-488 Tf endocytosis and clathrin protein levels in MES cells transfected with clathrin siRNA (b). Images as in (c). Bar represents 10 μm.

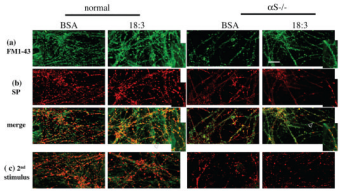

Fig. 8. Reduced FM1-43 internalization into synaptic vesicles and reduced synaptic pool in αS −/− primary hippocampal neurons

Hippocampal primary cultures (at 18 days) of normal and αS −/− mouse brains were conditioned for 16 hours in serum-free medium supplemented with BSA +/− 50 μM 18:3. (a) αS expression and PUFA treatment activate SV endocytosis. Fluorescence image after exposure to 10 μM FM1-43 in 90 mM K^+ solution for 60 s, followed by washout. White arrow represents the area of the inset. Bar represents 50 μM. (b) icc with anti synaptophysin ab (DAKO) performed on slides from (a). (c) Fluorescence image of cultures treated as in (a), after a second stimulation with 70 mM K^+ (FM1-43 download). (d) αS expression and PUFA treatment induced constitutive internalization of FM1-43 into neuronal cell bodies. Bar represents 25 μM. Fluorescent images as in (a and b) but without chemical stimulation.

Table 1

FM1-43 internalization as a function of FA carbon chain length and level of unsaturation

FA	FM1-43 internalization[1]
BSA	6.86 ± 1.7[2]
18:0 stearate	0.33 ± 0.12*
18:1 oleate	7.3 ± 0.941
18:2 linoleate	18.7 ± 1.2*
18:3 linolenate	27.5 ± 2.7*
20:0 arachidate	0.4 ± 0.2*
20:1 Eicosenoate	13.6 ± 1.67*
20:2 Eicosadienoate	22.3 ± 3.87*
20:3 eicosatrienoate	30.6 ± 3.89*
20:4 arachidonate	45.9 ± 2.67*

[1] see Methods for quantification of FM1-43 signal

[2] mean of (15–20 representative cells) ± SE

* $p < 0.05$, T-test vs. BSA alone,

Table 2

Quantification of synaptophysin-positive synapses and FM1-43 uptake in primary hippocampal neurons from wt and αS −/− mouse brains exposed to PUFA or not.

	wt-BSA	wt-PUFA	αS −/− BSA	αS −/− PUFA
FM1-43[1,2]	9.13 ± 1.78[2]	19.75 ± 7.1	2.25 ± 1.2	6.31 ± 2.45
Synaptophysin[1,2]	15.71 ± 2.78	18.53 ± 7.64	6.33 ± 2.3	6.83 ± 3.41

[1] quantification was done on microscopic fields containing highly similar neuritic densities and measured as signal above threshold and presented as % area.

[2] means ± SD of 7–9 fields for each treatment